IOSR Journal of Engineering (IOSRJEN) **www.iosrjen.org**
ISSN (e): 2250-3021, ISSN (p): 2278-8719
PP 01-06

Extraction of lumen region from OCT images of arteries using active contours

Aswini Narayanan[1],Nair Rohit Ramesh[2],Venkitaselvi[3],Vipin R[4]
(Department of Electrical and Electronics Engineering, Muthoot Institute of Technology & Science / Mahatma Gandhi University , India)

Abstract: *Optical Coherence Tomography (OCT) is gaining momentum in the field of medical imaging and disease identification due to its several advantages over the conventional ultrasound and X-ray imaging techniques. The analysis of the numerous images obtained using OCT however is considered to be an expert's job which makes the analysis cumbersome and more prone to errors. In this paper, we employ a different methodology of image segmentation technique using the second derivative approach for the extraction of lumen area in intravascular OCT images using active contours. Active contour is an active method in image processing that has been widely used for several automated image segmentation processes which use the minimal energy function to detect the boundaries of objects in an image. This property of active contours has been used in our work to detect the lumen boundary and separate it from the artery wall. We also demonstrate the performance of the proposed method in MATLAB with the collected OCT images of arteries.*

I. Introduction

Imaging methodologies and techniques have grown from infancy to maturity over the past 110 years. Modern technologies such as multi detector computed tomography, magnetic resonance imaging, dual-source computed tomography, microbubble enhanced ultrasound, etc. provide information based on pathology at higher resolutions, generating more information required for every day clinical practice[1]. Atheromatosis is a disease which can affect most of the arteries in a human body. This represents the cardiovascular syndromes and is a disease characterized by atheromatous degeneration of arteries. Digital subtraction angiography (DSA) is the modern standard in imaging and assessing the cardiovascular system which provides insights in vascular patency. It also introduces a tool to evaluate and analyze the direct results of intravascular interventional procedures. Its main defect is the inability to depict the vascular geometry in three dimensions and to provide adequate details about the vascular wall. These limitations are overcame by means of emerging of new imaging modalities like the rotational angiography systemsproviding adequate three dimensional information of the vasculature, as well as intravascular ultrasound (IVUS) and optical coherence tomography (OCT) systems [2].
The OCT image analysis is performed by human operators at present. The luminal boundary detection, the stent strut position, and the distance from the stent strut to the vessel wall are measured manually. However, it is very laborious and time-consuming and there will be issues related to the terms of intra- and inter-observer variability. The advancements in the Fourier-domain OCT technologies have increased the frame rates of imaging techniques from a few frames per second to more than 100 frames/sec. The increased number of frames however produces an increased chance of errors and a higher processing time for manual detection of diseased arteries. Thus, the clinical implementation of such techniques thus seems to be less practical due to the increased processing time and higher error rates [3]. To reduce the human efforts in the process of OCT image analysis and disease identification, several algorithms for automated image analysis based on different methods have been developed and evolved through these years.

In this paper, we present a new approach based on second-derivative operators which acquires the local maxima or minima. This directly produces the centroid positions of small objects, such as stent struts, with high intensity that could be adopted in this method of boundary detection. Local region-based active contouring technique is also employed since it is more robust and less sensitive to image noises and artifacts for vessel border detection. Energy functional of contours is defined to separate the lumen region and the vessel wall, and the steepest decent method is applied to the energy functional. The proposed algorithm holds true and easier for numerical experiments using OCT images.

II. Literature Review

Coronary artery disease is a leading problem of countries. The formation of unstable plaque cause stenosis and the rupture of such plaque can lead to occlusion of the arteries. Intracoronary stent which is made up of wire mesh and is tube-like structure is deployed for the treatment of stenosis. It is designed to be inserted into a coronary vessel and acts as a support device to keep the vessel open. Post assessment of the stent strut

position and quantitative measurement of the stent strut coverage are of great importance for stent placement evaluation and follow up diagnosis is described by B.K. Kim [3]. Several biomedical methods are developed for this and the application of optical technologies like Optical Coherence Tomography (OCT) is gaining more and more significance due to its high resolution output images.OCT is a non-invasive modality for cross-sectional optical imaging. It is basically analogous to ultrasound imaging except that it uses near-infrared light instead of ultrasound and measures the time-delay of light back-reflected from within biological tissues.

The optical instruments used in the field of medicine today take advantage of the coherent properties of light. Most of the instruments that use lasers, the ultimate generators of coherent light, can be classified as incoherent optical systems because the focused laser beam serves mainly as a source of illumination or concentrated heat. One of the reasons why optical coherence tomography (OCT) has attracted the attention of engineers and scientists working in the photonics field is that uses the coherent properties of light prominently. Optical coherence tomography improves localization of the returned signal origin due to the much shorter wavelength of the imaging light when compared with ultrasound; hence OCT offers significantly improved resolution is illustrated by F. Prati[1].

White-light interferometry that led to the development of Optical Coherence-Domain Reflectometry (OCDR), a one-dimensional (1-D) optical ranging technique was a great leap in the development of this technique for the application in biomedical field. OCDR was developed originally for finding faults in fibre optic cables and network components but it could also be used to probe the eye and other biological tissues. OCT achieves its improved sectioning ability by exploiting the short temporal coherence of a broadband light source which enables the OCT scanners to image microscopic structures in tissue at depths beyond the reach of conventional bright-field and confocal microscopes. In the eye and the frog embryo probing depths exceeding 2 cm have been demonstrated in transparent tissues. In the skin and other highly scattering tissues, OCT can image small blood vessels and other structures as deep as 12 mm beneath the surface is explained in this paper by J. M. Schmitt [4]. An advantage that OCT has over high-frequency ultrasonic imaging is the competing technology that achieves greater probing depths with lower resolution and lower cost of the hardware on which OCT systems are based.

The analysis of OCT images is presently performed by human operators and it basically includes the detection of obstructions in the arteries which restricts the blood flow through them which leads to severe cardiac ailments such as arteriosclerosis. Such obstructions cause the shrinkage in the lumen region of the artery. The positioning of such lipid depositions and extent of shrinkage in the lumen region is necessary for identification of the stent positions.A novel deformable-model-based algorithm for fully automated detection of optic disk boundary in retinal fundus images improved the original snake in two aspects clustering and smoothing update. The contour points are first self-separated into edge-point group or uncertain-point group by clustering after each deformation, and these contour points are then updated by different criteria based on different groups. These are reviewed by O. Chutatape [5]. The ideal OCT in retinal can be used for the future development and applications in the identification of artery shrinking due to plaque deposition.

A large number of OCT studies have demonstrated successful measurements of malapposed stent struts and evaluations of stent neointimal coverage. S. Tsantis have used a segmentation method based on the Markov Random Field (MRF) model for lumen area identification while the textural and edge information derived from local intensity distribution and continuous wavelet transform (CWT) analysis together to extract the inner luminal contour[6].A new approach based on second-derivative operators for the lumen region segmentation from the OCT images has been analyzed in this project work. The proposed method gives information about the centroid positions of small objects, such as stent struts, with high intensity because the second-derivative operator captures a local maxima or minima. This could be used for the measurement of the lumen area of the artery as well as the border detection which is described by B.K. Kim [3].

III. Image Segmentation using active contours

The image segmentation technique become complex if the input images collected are poor in resolution, blurred and mixed pixels images. In this paper work novel segmentation methods with a distinction framework called active contours was proposed. Active contours or snakes are computer generated curves [7] which move within the image to find object boundaries under the influence of internal and external forces. Snakes model of active contour were proposed by Kass, which is considered as satisfactory for the occurrence of contour evolution technique. By finding contour C such that the energy E of snake can be minimized by setting and defining weights. In the first stage the snake points associated on the plane of image and the next location of snake points are determined by confined minimum E. The related form of snake spot is observed as the contour [8].

For calculating the energy of snake the following energy functional is introduced which is described in Eq(1):

$$E_{snake}=E_{internal}+E_{external}+E_{constraint} \quad (1)$$

Here $E_{internal}$ represents the internal energy of the snake, E_{img} represents the image forces, while $E_{constarint}$ provide rise to external constraint forces. The sum of all this is simply known as the external snake forces, represented by $E_{external}$ [8] . The Gradient Vector Flow is used to enhance the ability of the snake so that it can move into the boundary hollow and also to increase and improve capture ranges. There is limit in the capture range of the real snake at the place of the desired contour. In the hollow regions there has some problem of original snake. This problem can be rectified by introducing new external force the GVF to the existing original snake. By minimizing an energy function we can get a new vector field using this following external [9].

$$V(x,y)= (U(x,y),V(x,y)) \quad (2)$$

V(x,y) is described to the minimized energy which defined in the Eq(2).Level Set Method is used to keep original properties of the real image. The part of the image which is not necessary then it ignore that part of an image [10]. The level set method uses the speed function that helps to stop the motion when the boundary is achieved [11].

A. Region based active contour

Generally region-based active contour shape contains two components. One is the regularity in which the smooth form of contours is inside it. Other is the energy minimization part, which finds for the equality of a desired property within a sub-set. If the contour is located in anywhere in the image then it finds it quickly that it is good region based active contour. The region based active contour are associated with the overall energy minimization than that of the confined energy minimization[12].Compared to edge detection method, segmentation algorithms based on region are relatively simple and more immune to noise[13,14]. Edge based methods partition an image based on rapid changes in intensity near edges whereas region based methods, partition an image into regions that are similar according to a setof predefined criteria [15,16] .

IV. Proposed Methodology

For the detection of vessel lumen's border, we first remove the region around the centroids of the stent struts. Let 'c' be a curve dividing $\tilde{\Omega}$ into two regions, one above and the other below the curve 'c', denoted by $\tilde{\Omega}\_C$ and $\tilde{\Omega}_+C$, respectively. We also let p = (Θ, r) denote a position in Cartesian coordinates $\tilde{\Omega}$and $R_\rho(p)$be a square with side length 2ρ centred at **'p'.** We assign the vessel lumen and vessel tissue to the above and below regions of 'c', respectively. We developed a simple energy functional defined by, Eq(3).

$$E(C) = |C| + \lambda \int_c f(p)\left[A_p - A_+(p)\right]ds \quad (3)$$

Where |c| is the arc-length of 'c' , λ is a fitting parameter , and A_- and A_+ are the average intensity values given by A_p = average of $\widetilde{I_\sigma}$ over $\{\Omega\_(c) \cap R_\rho(p)\}$ andA_+p = average of $\widetilde{I_\sigma}$ over $\{\Omega_+(c) \cap R_\rho(p)\}$ for the square $R_\rho(p)$ respectively .f(p) is defined as gradient based function. In this energy functional in equation (3), the first is a regularization term to penalize for the non-smoothness of 'c', and the second term is a fitting term to attract the curve 'c'toward the border of the vessel. When the contour 'c'is located at the border of the vessel, the$[A_(p) - A + (p)]$of the second term is minimized with the minus sign because the average intensity in the vessel's lumen is smaller than the average intensity in the vessel's tissue. Here, $f(p)$plays the role of amplifying the$[A_(p) - A + (p)]$ for *C*, located at the vessel's border. We do not take the square of the quantity $[A\_(p) - A + (p)]$ to prevent the wrong border detection in the vessel wall's region, where it has the plus sign. To reduce error due to speckles we use blood residuals and tissue heterogeneities, local regions.

$$\varepsilon(r_1, \dots\dots\dots, r_n) = \sum_{i=1}^{n} |p_{i+1} - p_i| + \lambda \sum_{i=1}^{n} f(p_i)\left(A \quad (p_i) - A_+(p_i)\right)$$

$$= \sum_{i=1}^{n} \sqrt{(\theta_{i+1} - \theta_i)^2 + (r_{i+1} - r_i)^2}$$

$$= \lambda \frac{1}{\rho(2\rho+1)} \sum_{i=1}^{n} f(\theta_i, r_i)\left(\sum_{j=-\rho}^{\rho} \sum_{k=1}^{\rho} [\tilde{I}_\sigma(\theta_i + j, r_i - k) - \tilde{I}_\sigma((\theta_i + j, r_i + k)]\right) \quad (4)$$

We let Dim$\theta(\tilde{\Omega})$ be the Θ- directional dimension of $\tilde{\Omega}$,we use the periodicity of the images on the Θ- axis $r_{n+1} + r_1$, and we assume that the curve 'c' locally flat for the second identity in Eq.(4). To compute the minimizer of Eq(4) , we derive the Euler-lagrange equation that can be obtained by taking the partial derivative of E with r_i.

$$\frac{\partial \varepsilon(r_1, \dots\dots r_n)}{\partial r_i} = \frac{r_i - r_{i+1}}{\sqrt{(\theta_{i+1} - \theta_i)^2 + (r_{i+1} - r_i)^2}} + \frac{r_i - r_{i-1}}{\sqrt{(\theta_i - \theta_{i-1})^2 + (r_i - r_{i-1})^2}}$$

$$= \lambda \frac{1}{\rho(2\rho+1)} \left\{ \frac{\partial f}{\partial r}(\theta_i, r_i) \left(\sum_{j=-\rho}^{\rho} \sum_{k=1}^{\rho} [\tilde{I}_\sigma(\theta_i + j, r_i - k) - \tilde{I}_\sigma((\theta_i + j, r_i + k)] \right) \right.$$

$$\left. + \mathrm{f}(\theta_i, r_i) \left(\sum_{j=-\rho}^{\rho} \sum_{k=1}^{\rho} \left[\frac{\partial \tilde{I}_\sigma}{\partial r}(\theta_i + j, r_i - k) - \frac{\partial \tilde{I}_\sigma}{\partial r}(\theta_i + j, r_i + k) \right] \right) \right\}$$

$$= \cos(< p_{i+1}\, p_i p'_{i+1}) + \cos(< p_{i-1}\, p_i p'_{i-1}) + \lambda \left\{ \frac{\partial f}{\partial r}(p_i) \left(A_{\_}(p_i) - A_{+}(p_i) \right) + f(p_i) \frac{\partial}{\partial r} \left(A_{\_}(p_i) - A{+}pi \quad (5) \right. \right.$$

where p'_{i-1} and p'_{i+1} are the projected points of p_{i+1} and p_{i-1} on the A- line passing through p_i, respectively , and $< p_{i-1}p_i p_{i-1}$ is the angle between the segments $p_{i-1}p_i$ and $p_i p'_{i-1}$. From the first term of the second identity, we can infer that a severely-distorted curve produces a non-zero force while a flat curve does not generate force. The second term becomes zero if the curve is located on the vessel' s border. Then the Euler-lagrange equation is Eq(6)

$$0 = \frac{\partial \varepsilon(r_1, \ldots\ldots\ldots r_n)}{\partial r} = \left(\frac{\partial \varepsilon}{\partial r_1}, \ldots \ldots \ldots, \frac{\partial \varepsilon}{\partial r_n} \right) \qquad (6)$$

and this leads to the steepest-descent direction with a minus sign ($\frac{-\partial E}{\partial r}$) We apply the steepest-descent method to minimize the energy ie, Eq(7)

$$\left[r_1^{(k+1)}, \ldots \ldots \ldots, r_n^{(k+1)} \right] = \left[r_1^{(k)}, \ldots \ldots \ldots, r_n^{(k)} \right] - \Delta t \left[\frac{\partial \varepsilon(r_1^{(r)}, \ldots \ldots, r_n^{(k)}}{\partial} \right] \quad (7)$$

Where Δt is a time step , and the superscripts (k) and (k+1) refer to the k and the k+1 iterations , respectively . In this case, the computation of Eq(3) does not produce the correct vessel border , as it is mainly influenced by the image noise in the shadow region On the other hand , if the radius is too large , image artifacts such as blood residuals and irregular vessel features, which result in inaccurate measurements, may also be included. We, therefore, chose the side length of $R_\rho(p)$ to be twice the average width of the stent shadows. For the optimal parameter λ , we define the quantity $\tilde{\iota}$ as a function of p_i for all I as Eq(8)

$$\tilde{\iota} = \sqrt{\frac{\sum_{i=1}^{n} || \cos(< p_{i+1} p_i p'_{i+1}) + \cos(< p_{i-1} p_i p'_{i-1}) ||^2}{\sum_{i=1}^{n} \left| \frac{\partial f}{\partial r}(p_i) \left(A_{\_}(p_i) - A_{+}(p_i) \right) + f(p_i) \frac{\partial}{\partial r} \left(A_{\_}(p_i) - A_{+}(p_i) \right) \right|^2}} \qquad (8)$$

This is derived from Eq(5) and Eq(6) . We note that if p_i satisfies Eq(6) for all i=1 ,……n, $\tilde{\iota} = \lambda$ One can see that quantity $\tilde{\iota}$ depends on the smoothness of the curve 'c' and the intensity difference between the lumen and vessel tissue . The regularization parameter λ was empirically determined by using the training set images. The images of the training sets were used to manually trace the vessel contours were then used to evaluate Eq(8) from which the optimal λ was determined as the mean value of the calculated $\tilde{\iota}$s.

V. Simulation Results

The input OCT image is converted to grayscale images and then the initial contour is specified. Initial contour is the location at which the evolution of the segmentation begins and is specified on grayscale images of same size as the input image. For 2-D and 3-D grayscale images, the size of mask must match the size of the input image. For colour and multichannel images, mask must be a 2-D logical array where the first two dimensions match the first two dimensions of the input image. Maximum number of iterations to perform in evolution of the segmentation is specified as a numeric scalar. The contour stops the evolution of the active contour when it reaches the maximum number of iterations. If the initial contour position (specified by mask) is far from the object boundaries, specify higher values to achieve desired segmentation results.

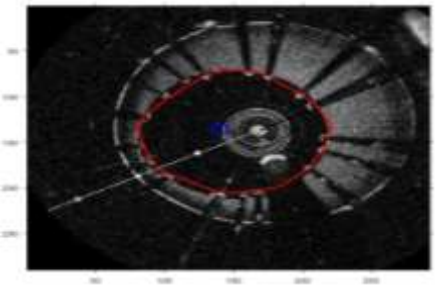

Figure 1: Image with initial and final contour

The average intensity of the lumen region is less than the average intensity of the vessel tissue. Hence the difference in the intensity will be the maximum at the boundary between the lumen and the vessel tissue. The second derivative of the energy function will be negative maximum where the difference in intensities is the maximum. Thus the points at the boundaries can be traced. These points when joined together will fetch us the lumen boundary. Once the lumen boundary is detected the lumen region is segmented out from the actual image and the area of the lumen is calculated.

The image boundary detection algorithm applied on the OCT data that we had collected is shown in fig. 1. The red curve indicates the boundary of the lumen region that was developed using our technique. The blue spot indicates the initial contour. As the number of iterations varies the contour size varies and it fits the minimal energy lumen boundary at the end of the iteration. The contour is made to expand towards the lumen boundary from the initial contour specified.

VI. Conclusion

The quality and accuracy of segmentation is often affected by the characteristics of the input image. Noise and other disturbances may lead to inefficient results which could be eliminated using several pre-processing techniques. Development and implementation of a graphical interface that is user friendly with an optimized programming scheme for deployment on a larger-scale evaluation are currently underway. An algorithm and MATLAB code implementation of the lumen boundary identification and extraction of lumen region from the intravascular OCT images of arteries was carried out as a part of this work. The results were encouraging which motivates the use of such automated processes for image analysis replacing human efforts. This technique can be extended as a valuable tool for physicians to identify and for the quantitative analysis of stent endothelialisation in clinical OCT datasets of human arteries.

VII. Future Works

The efficient medical image segmentation using region based segmentation of active contours on OCT images was resulted.

I. This technique avoided the need for manual selection of the suspected region window, seed pixel and threshold value processes.

II. In addition, this technique evaluates the findings by proven statistical technique to authenticate the accuracy of detection methods.

III. These methods are used for other medical image processing applications with minor modification.

The proposed technique is acceptably accurate, promising and comparable with any other standard methods and in future the works aim in attaining higher accuracy. A further extension, the technique is applied to a benchmark data sets extracted from various research repositories. Various researches concentrates on different aspects such as authentication of medical image processing and on handling the limitations in the algorithm, such as improving its performance foe texture images and video sequences with a relatively large camera motion.

References

[1]. F. Prati, E. Regar, G. Mintz, E. Arbustini, C. Di Mario, I. Jang, T. Akasaka, M. Costa, G. Guagliumi, E. Grube, Y. Ozaki, F. Pinto, and P. Serruys, "Expert review document on methodology, terminology, and clinical applications of optical coherence tomography: Physical principles, methodology of image acquisition, and clinical application for assessment of coronary arteries and atherosclerosis," European Heart Journal, vol. 31, no. 4, pp. 401–415, 2 2010.

[2]. A. F. Low, G. J. Tearney, B. E. Bouma, and I. K. Jang, "Technology Insight: Optical coherence tomography—Current status and future development,"Nat. Clin. Pract. Cardiovasc. Med. 3, 154–162 ,2006.

[3]. C. Y. Ahn, B.-K. Kim, M.-K. Hong, Y. Jang, J. Heo, C. Joo, and J. K. Seo, "Automated measurement of stent strut coverage in intravascular optical coherence tomography," Journal of the Korean Physical Society, vol. 66, no. 4, pp. 558–570, Feb 2015.

[4]. J. M. Schmitt, "Optical coherence tomography (oct): a review," IEEE Journal of Selected Topics in Quantum Electronics, vol. 5, no. 4, pp. 1205–1215, Jul 1999.

[5]. J. Xu, O. Chutatape, and P. Chew, "Automated optic disk boundary detection by modified active contour model," IEEE Transactions on Biomedical Engineering, vol. 54, no. 3, pp. 473–482, March 2007.

[6]. S. Tsantis, G. Kagadis, K. Katsanos, D. Karnabatidis, G. Bourantas, and G. Nikiforidis,"Automatic vessel lumen segmentation and stent strut detection in intravascular optical coherence tomography," vol. 39, pp. 503–13, 01 2012.

[7]. X. Jiang, R. Zhang, S. Nie,"Image Segmentation Based on PDEs Model: a Survey", IEEE conference, pp. 1-4, 2009.

[8]. E., Mendi, M., Milanova , "Contour-Based Image Segmentation Using Selective Visual Attention", In: J. Software Engineering & Applications, Vol. 3,pp. 796-802, 2010.

[9]. C., Xu, J.L., Prince, "Snakes, Shapes, and Gradient Vector Flow", In: IEEE transactions on image processing, Vol. 7, No.3, 1998,ISSN:1057-7149.

[10]. D. Jayadevappa, S. Srinivas Kumar, and D. S. Murty, "A Hybrid Segmentation Model Based on Watershed and Gradient Vector Flow for the Detection of Brain Tumor", In: International Journal of Signal Processing, Image Processing and Pattern Recognition, Vol. 2, No.3, pp.29-42, 2009.

[11]. Md. G. Moazzam , A. Chakraborty , S., Nasrin , and M., Selim, "Medical Image Segmentation Based on Level Set Method" , In: IOSR Journal of Computer Engineering (IOSR-JCE), Vol. 10,No. 6, pp. 35-41, 2013,ISSN:2278-0661.

[12]. T., Liu, H., Xu, W., J. Z., Liu, Y., Zhao, W., Tian, " Medical Image Segmentation Based on a Hybrid Region-Based Active Contour Model" In:proceeding of Hindawi Publishing Corporation, Vol 2013, pp. 1-10, 2014.
[13]. W. X. Kang, Q. Q. Yang, R. R. Liang,"The Comparative Research on Image Segmentation Algorithms", IEEE Conference on ETCS, pp. 703-707, 2009.
[14]. H. Zhang, J. E. Fritts, S. A. Goldman,"Image Segmentation Evaluation: A Survey of unsupervised methods", computer vision and image understanding, pp. 260-280, 2008.
[15]. H. G. Kaganami, Z. Beij,"Region Based Detection versus Edge Detection", IEEE Transactions on Intelligent information hiding and multimedia signal processing, pp. 1217-1221, 2009.
[16]. Rafael C. Gonzalez, Richard E. Woods, "Digital Image Processing", 2nd ed., Beijing: Publishing House of Electronics Industry, 2007.